

ROCK FAILURE IN COMPRESSION

S.Nemat-Nasser and H.Horii

Department of Civil Engineering
The Technological Institute
Northwestern University
Evanston, Illinois 60201

ABSTRACT

Mechanisms of rock failure in compression -- axial splitting and shear failure -- are studied, based on a microscopic consideration. Analytical models are constructed and model experiments on plates of a brittle polymer are performed. It is shown that unstable growth of tension cracks which propagate from the tips of pre-existing cracks and curve towards the maximum compressive direction, is the fundamental mechanism that produces axial splitting of a uniaxially compressed rock specimen, whereas shear failure of a triaxially compressed specimen is a result of sudden growth of tension cracks at tips of a suitably arranged interacting set of microcracks. The simultaneous out-of-plane unstable growth of a suitably oriented row of cracks is analyzed and, on the basis of this model, the variations of the "ultimate strength" and the orientation of the overall fault plane with the confining pressure are estimated. The brittle-ductile transition is discussed with the aid of a model which includes both tension crack extension and plastic zone development from the pre-existing cracks.

1 INTRODUCTION

Brittle solids such as rock and concrete by their nature contain numerous microcracks and inhomogeneities. Materials of this kind fail under uniaxial compression by axial splitting, where the fracture surface is parallel to the axial compression direction. Shear failure, on the other hand, is observed under triaxial compression; Peng and Johnson (1972). The ultimate strength and the orientation of the macroscopic failure plane depend on the confining pressure in a complex manner. Generally speaking, the strength versus confining pressure curve is non-linear under low confining pressures and is almost linear under moderate confining pressures; Mogi (1966). The inclination of the overall failure plane relative to the compression axis increases with increasing confining pressure, almost attaining the constant value of 30° under moderate confining pressures. In the brittle-ductile transition stage, plastic flow takes place along the failure plane; Griggs and Handin (1960).

Based on the idea that frictional sliding on pre-existing cracks results in the formation of tension cracks at their tips, models for microcracking under compression have been proposed; e.g., Brace and Bombolakis (1963) and McClintock and Walsh (1963). Nemat-Nasser and Horii (1982) present an analytical solution of compression-induced, out-of-plane crack extension, and study the mechanism of the axial splitting; see also Horii and Nemat-Nasser (1983a,b) and Nemat-Nasser (1983). Their results are summarized in Section 2.

Photographic studies of Hallbauer, Wagner and Cook (1973) show that under triaxial compression the microcrack distribution is almost uniform until the applied stress reaches the ultimate strength, and at the ultimate strength a region of high crack-density (tension cracks) emerges along a plane which eventually becomes a macroscopic shear failure plane. To reveal the mechanism of shear failure, Horii and Nemat-Nasser (1983b) consider a row of suitably oriented cracks, and examine their simultaneous out-of-plane unstable growth which may lead to possible macroscopic faulting. They estimate the variations of the "ultimate strength" and the orientation of the overall failure plane with confining pressure, using this model. These results are presented in Section 3.

As the confining pressure increases, the transition from brittle to ductile behavior is observed, where plastic flow occurs along the failure plane; Griggs and Handin (1960). Edmond and Paterson (1972) report that dilatancy persists well in this range. Following this observation and the results of our model experiments, a model for the mechanism dominant in the brittle-ductile transition range, which includes both the tension crack extension and the plastic zone development from the pre-existing cracks, is proposed in Section 4.

2 AXIAL SPLITTING

Under axial compression, a pre-existing crack undergoes frictional sliding which leads to the formation of tension cracks at its tips. The tension cracks grow at sharp angles relative to the orientation of the pre-existing crack and curve into a direction parallel to the maximum compressive direction. This is

illustrated in Fig. 1 which shows kinked-curved cracks at the tips of a pre-existing crack in an axially compressed plate of Columbia Resin CR36. This is considered to be the mechanism of microcracking under compression; Brace and Bombolakis (1963), Hoek and Bieniawski (1965), and Nemat-Nasser and Horii (1982).

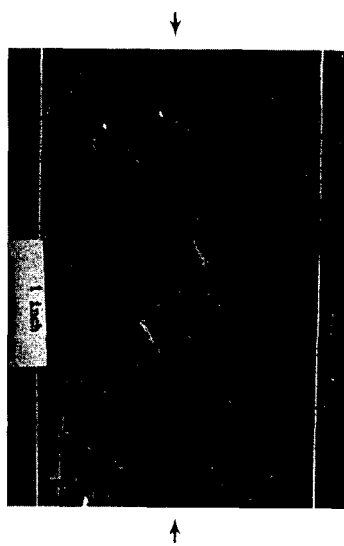


Fig.1 Kinked-curved crack extension from the tips of a pre-existing crack.

An analytic solution for the problem of out-of-plane curved crack growth, illustrated in Fig. 2, is obtained by Nemat-Nasser and Horii (1982); see also Nemat-Nasser (1983) and Horii and Nemat-Nasser (1983a,b).

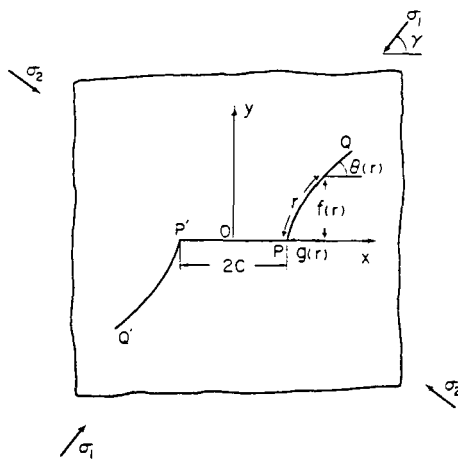


Fig.2 Pre-existing crack PP' and its extensions PQ and $P'Q'$.

The calculated crack profiles are compared with those observed on model experiments; Fig. 3. The most significant result is the variation of the axial load versus crack extension length curve with the lateral stress; see Fig. 4. Under axial compression with lateral compression, crack growth is stable and stops

at a certain finite length. In the presence of small lateral tension, on the other hand, crack growth becomes unstable after a certain crack extension length is attained. This unstable crack growth is considered to be the fundamental mechanism which produces axial splitting of a uniaxially compressed rock specimen. Peng and Johnson (1972) report the presence of lateral tension in the uniaxially compressed specimen because of the end-boundary conditions. Different inserts affect the ultimate strength; the normalized strength becomes 9.5 for the steel insert, 7.3 for the teflon insert, and 5.9 for the neoprene insert. They also report a radial tensile stress of 6-8% of applied compression for the neoprene insert, and 4-6% for the teflon insert. These experimental data seem to support our analytical results.

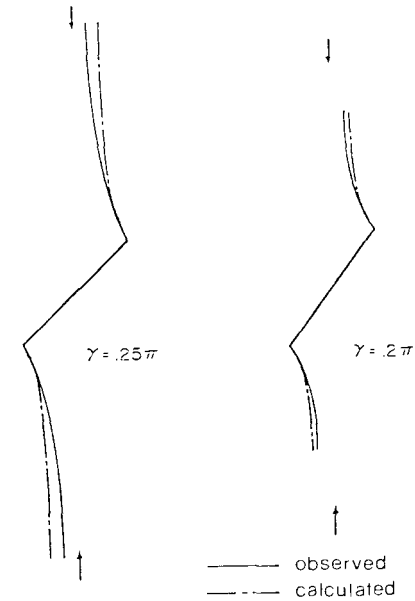


Fig.3 Calculated and observed crack profiles; Horii and Nemat-Nasser (1983b).

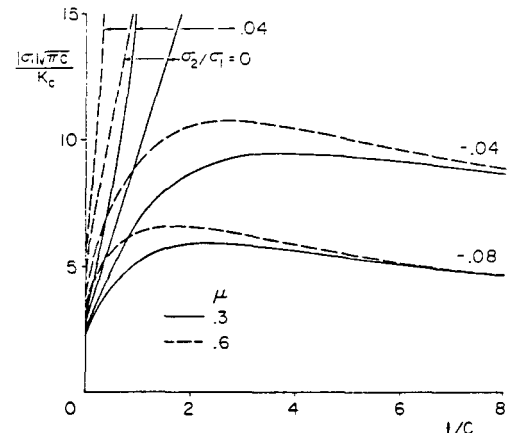


Fig.4 Normalized axial compression required to attain the associated crack extension length; Horii and Nemat-Nasser (1983b).

3 SHEAR FAILURE

A rock specimen contains microcracks of various sizes. Smaller cracks are greater in number and closer in spacing. Under axial compression, larger cracks become activated first. Without lateral confinement, they continue to grow, leading to axial splitting; Fig. 5. In the presence of lateral compression, on the other hand, their growth is soon arrested and, at a certain stress level, suitably oriented smaller cracks become activated because of their interaction. Then a narrow zone containing many microcracks is formed, which eventually becomes a macroscopic failure plane; Fig. 6.

Based on observations by Hallbauer *et al.* (1973) and our model experiments, it appears

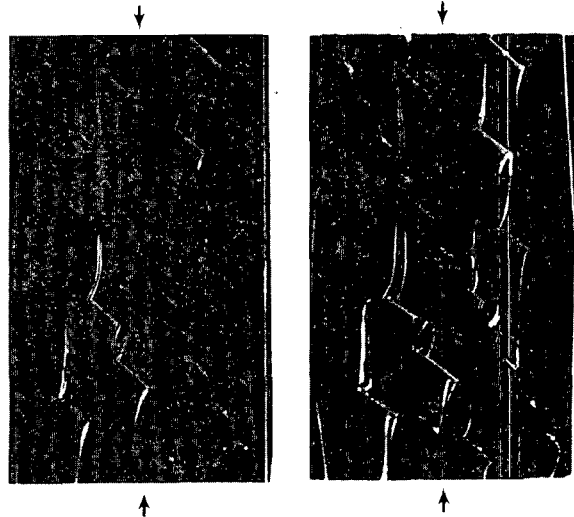


Fig.5 The axial splitting of the specimen under uniaxial compression; Horii and Nemat-Nasser (1983b).

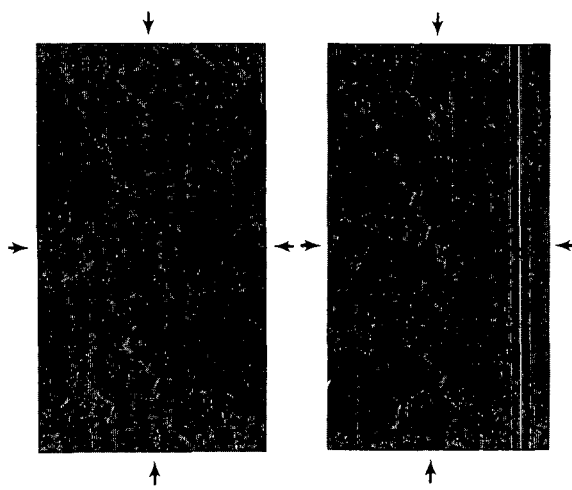


Fig.6 Unstable growth of tension cracks at tips of a row of interacting pre-existing cracks under triaxial compression; Horii and Nemat-Nasser (1983b).

that shear failure may be considered to be the result of unstable growth of a suitably oriented set of interacting pre-existing cracks. To capture this feature, Horii and Nemat-Nasser (1983b) consider a row of equally spaced cracks of equal initial size and of common orientation; see Fig. 7. The required axial compression is calculated as a function of the crack extension length for constant confining pressure. Typical results are shown in Fig. 8.

For small values of ϕ of Fig. 7, the axial compression first increases with increasing crack extension length, attains a peak value,

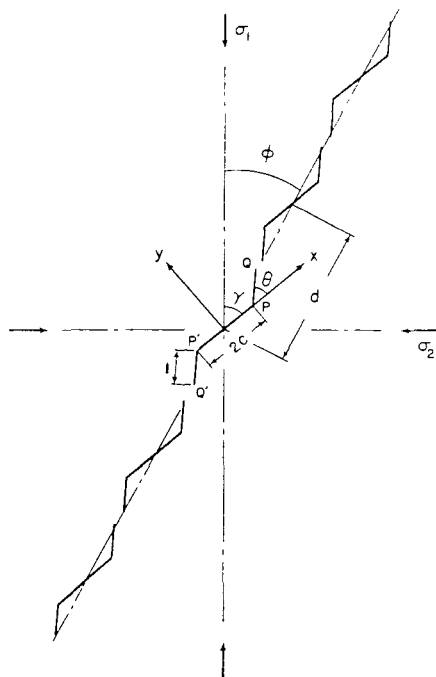


Fig.7 An infinite plate with a row of pre-existing cracks and their out-of-plane extensions.

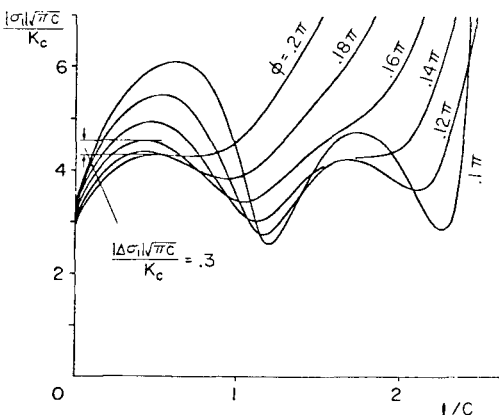


Fig.8 Axial stress versus crack extension length: $\gamma = .24\pi$ and the coefficient of friction $\mu = .4$; Horii and Nemat-Nasser (1983b).

decreases, and then begins to rise again. This suggests an unstable growth of optimally oriented cracks at a critical value of the axial stress, which is considered to correspond to the formation of a fault zone. It is seen from Fig. 8 that the peak values of the axial stress for the values of ϕ from 0.16π to 0.2π fall in a very narrow range, i.e. $|\Delta\sigma_1|/\sqrt{\pi c}/K_c \sim 0.3$. This implies that the overall failure angle is sensitive to imperfection and other effects. Indeed, the orientation of the fracture plane observed in experiments often scatters over a wide range. The range of the overall failure angle, however, may be limited since the peak value of the axial stress increases sharply as ϕ decreases. We can specify the possible range of the overall orientation angle ϕ by prescribing the "stress barrier" $|\Delta\sigma_1|/\sqrt{\pi c}/K_c$ which can be overcome. The value of γ of Fig. 7 is chosen such that the required axial compression for the instability is minimized.

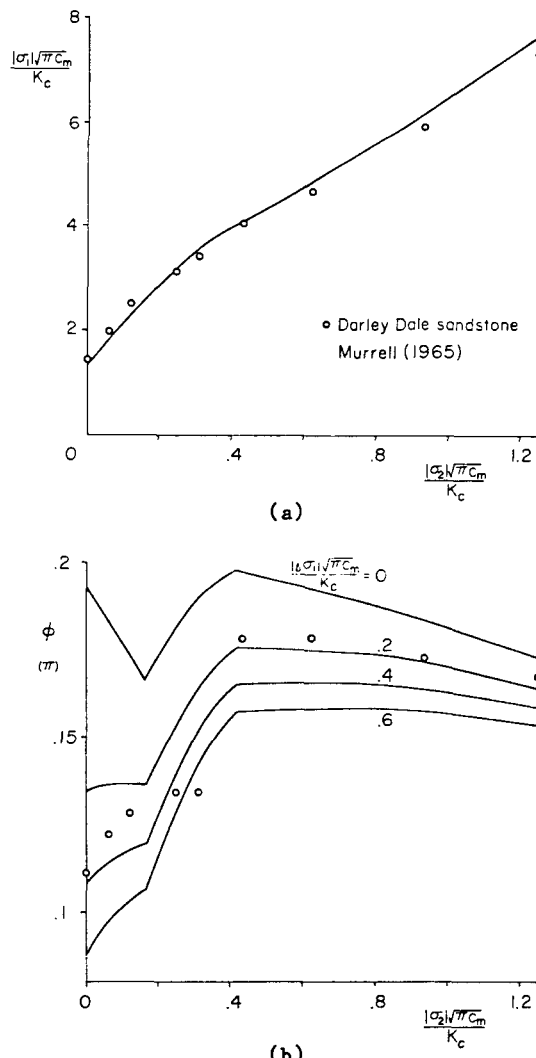


Fig.9 Variations of (a) the ultimate strength, (b) overall failure angle with the confining pressure; Horii and Nemat-Nasser (1983b).

Now we can calculate the critical axial load, $|\sigma_1|/\sqrt{\pi c}/K_c$, and the possible range of the overall failure angle, ϕ , for a given confining pressure and crack spacing d/c . In the actual rock specimen, there are many cracks of various sizes. It is reasonable to expect that smaller cracks are greater in number and closer in spacing. Thus, one may assume that the spacing of the "optimally oriented" cracks is an increasing function of the crack size. We, therefore, introduce the simple relation,

$$d/c_m = b(c/c_m)^{1+a}, \quad b = d_m/c_m, \quad a > 0,$$

where c_m and d_m denote the minimum crack size and the corresponding crack spacing, and a and b are constants. With this relation we can calculate the ultimate strength which is the minimum of the axial critical load and the possible range of the overall failure angle as functions of the confining pressure. Typical results are shown in Figs. 9a,b with $d_m/c_m = 3.0$, $a = 0.18$, and $K_c/\sqrt{\pi c_m} = 8 \times 10^3$ psi. The corresponding experimental data on Darley Dale sandstone reported by Murrell (1965) are also shown in these figures.

4 BRITTLE-DUCTILE TRANSITION

The model of brittle fracture discussed in Section 3 anticipates that the critical load for instability increases with increasing confining pressure. This is shown in Fig. 10, where the relation between the axial load and the crack extension length is plotted for different values of the confining pressure. Whereas at lower confining pressures the curves have distinct peaks, at higher pressures the peaks disappear. This suggests that the brittle fracture model discussed in Section 3 is no longer applicable at high confining pressures.

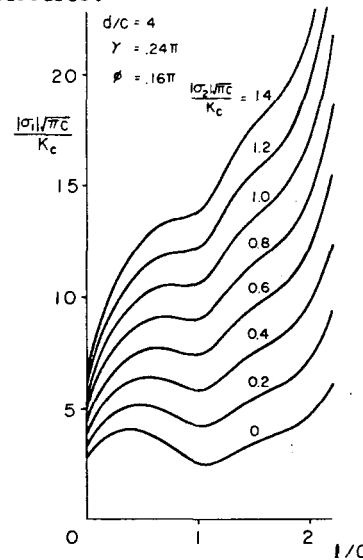


Fig.10 The axial load versus crack extension length curve for indicated values of the confining pressure.

In the brittle-ductile transition stage, plastic flow occurs along the failure plane; Griggs and Handin (1960). However, Edmond and Paterson (1972) report that dilatancy persists well in this range. Since dilatancy results from microcracking, it may be concluded that both microcracking and plastic flow occur in the brittle-ductile transition stage.

The photoelastic picture of Fig. 11 shows the residual strains in the unloaded specimen (shown in Fig.6). It illustrates the development of plastic zones after biaxial compression of the plate which contains pre-existing cracks.



Fig.11 The residual strains in the unloaded specimen of Fig.6.

In the brittle-ductile transition stage, the development of the plastic zones, and their interaction are considered to be the controlling mechanism of the overall deformation. A model which includes tension cracks and plastic zones at the tips of the pre-existing cracks is now being investigated by the present authors.

ACKNOWLEDGMENT

This work has been supported by the U.S. Air Force Office of Scientific Research grant AFOSR-84-0004 to Northwestern University.

REFERENCES

Brace, W.F., and E.G. Bombolakis (1963), "A note on brittle crack growth in compression", *J. Geophys. Res.*, **68**(12), 3709-3713.

Edmond, J.M., and M.S. Paterson (1972), "Volume changes during the deformation of rocks at high pressures", *Int. J. Rock Mech. Min. Sci.*, **9**, 161-182.

Griggs, D., and J. Handin (1960), "Observations on fracture and a hypothesis of earthquakes", *Rock deformation* (edited by D. Griggs and J. Handin), *Mem. Geol. Soc. Am.*, **79**, 347-364.

Hallbauer, D.K., H. Wagner, and G.W. Cook (1973), "Some observations concerning the microscopic and mechanical behaviour of quartzite specimens in stiff, triaxial compression tests", *Int. J. Rock Mech. Min. Sci. & Geomech. Abstr.*, **10**, 713-726.

Hoek, E., and Z.T. Bieniawski (1965), "Brittle fracture propagation in rock under compression", *Int. J. Fract. Mech.*, **1**, 137-155.

Horii, H., and S. Nemat-Nasser (1983a), "Estimate of stress intensity factors for interacting cracks", *Advances in Aerospace Structures, Materials and Dynamics, AD-06*, ASME, 111-117.

Horii, H., and S. Nemat-Nasser (1983b), "Compression-induced micro-crack growth in brittle solids: axial splitting and shear failure"; submitted to *J. Geophys. Res.*.

McClintock, F.A., and J.B. Walsh (1963), "Friction on Griffith cracks in rocks under pressure", *Proc. 4th U.S. Nat. Congr. Appl. Mech. 1962*, ASME, New York, **2**, 1015-1021.

Mogi, K. (1966), "Pressure dependence of rock strength and transition from brittle fracture to ductile flow", *Bull. Earthquake Res. Inst.*, **44**, 215-232.

Murrell, S.A.F. (1965), "The effect of triaxial stress systems on the strength of rocks at atmospheric temperatures", *Geophys. J. Roy. Astr. Soc.*, **10**, 231-281.

Nemat-Nasser, S. (1983), "Non-coplanar crack growth", *Proc. ICE Int. Symp. on Fract. Mech.*, Beijing, China, Nov. 22-26, 185-197.

Nemat-Nasser, S., and H. Horii (1982), "Compression-induced nonplanar crack extension with application to splitting, exfoliation, and rockburst", *J. Geophys. Res.*, **87**(B8), 6805-6821.

Peng, S.D., and A.M. Johnson (1972), "Crack growth and faulting in cylindrical specimens of Chelmsford granite", *Int. J. Rock Mech. Min. Sci.*, **9**, 37-86.